International Journal of Nanomedicine

Dovepress
open access to scientific and medical research

Open Access Full Text Article

ORIGINAL RESEARCH

Vertical Guided Bone Regeneration in the Rabbit Calvarium Using Porous Nanohydroxyapatite Block Grafts Coated with rhVEGF$_{165}$ and Cortical Perforation

This article was published in the following Dove Press journal:
International Journal of Nanomedicine

Weizhen Liu[1,*]
Bing Du[2,*]
Siyi Tan[3]
Qin Wang[4]
Yi Li[1]
Lei Zhou[5]

[1]Department of Periodontics, School of Stomatology, Southern Medical University, Guangzhou, Guangdong, People's Republic of China; [2]Center of Stomatology, The Second People's Hospital of Foshan, Foshan, Guangdong, People's Republic of China; [3]Center of Stomatology, Panyu Central Hospital, Guangzhou, Guangdong, People's Republic of China; [4]Department of Oral Maxillofacial Surgery, School of Stomatology, Southern Medical University, Guangzhou, Guangdong, People's Republic of China; [5]Center of Oral Implantology, School of Stomatology, Southern Medical University, Guangzhou, Guangdong, People's Republic of China

*These authors contributed equally to this work

Introduction: Vertical bone augmentation without osseous walls to support the stability of clots and bone grafts remains a challenge in dental implantology. The objectives of this study were to confirm that cortical perforation of the recipient bed is necessary and to evaluate whether nanohydroxyapatite (nHA) block grafts coated with recombinant human vascular endothelial growth factor$_{165}$ (rhVEGF$_{165}$) and cortical perforation can improve vertical bone regeneration.

Materials and Methods: We prepared nHA blocks coated with or without rhVEGF$_{165}$ on the rabbit calvarium through cortical perforation, and designated the animals as the non-perforated group (N-nHA), rhVEGF$_{165}$ group (NV-nHA), perforated group (P-nHA) and rhVEGF$_{165}$ on perforated group (PV-nHA). Micro-computed tomography (micro-CT) and fluorescence microscopy were selected to evaluate parameters of vertical bone regeneration at 4 and 6 weeks.

Results: The ratio of the newly formed bone volume to the titanium dome volume (BV/TV) and the bone mineral density (BMD) were significantly higher in the PV-nHA group than in the N-nHA group at 4 and 6 weeks, as determined using micro-CT. The fluorescence analysis showed slightly greater increases in new bone regeneration (NB%) and vertical height (VH %) gains in the P-nHA group than in the N-nHA group. Greater increases in NB% and VH% were observed in groups treated with rhVEGF$_{165}$ and perforation than in the blank groups, with significant differences detected at 4 and 6 weeks (N-nHA compared with PV-nHA, $p<0.05$). A greater VH% that was observed at the midline of the block in the PV-nHA group than in the other three groups at both time points (0.75±0.53% at 4 weeks and 0.83±0.42% at 6 weeks).

Conclusion: According to the present study, cortical perforation is necessary and nHA blocks coated with rhVEGF$_{165}$ and decoration could work synergistically to improve vertical bone regeneration by directly affecting primary osteoblasts and promoting angiogenesis and osteoinduction.

Keywords: cortical perforation, vertical bone regeneration, hydroxyapatite blocks, fluorescence, angiogenesis

Plain Language Summary

Vertical bone augmentation remains a challenge in dental implantology. The block form of nanohydroxyapatite (nHA) is good at maintaining a sufficient amount of space, which is convenient to rebuild bone volume. However, insufficient vascularization in the central area and the low capacity for osteoinduction restrict its clinical application.

Correspondence: Lei Zhou
Center of Oral Implantology, School of Stomatology, Southern Medical University, Guangzhou, Guangdong 510280, People's Republic of China
Tel +86 20 8423 3801
Fax +86 20 8443 3177
Email zho668@263.net

submit your manuscript | www.dovepress.com
DovePress
http://doi.org/10.2147/IJN.S268182

In the present study, the rabbit calvarial model was an effective tool to evaluate vertical bone augmentation. Cortical perforation provided passageways for blood vessels and progenitor cells to accelerate bone augmentation, as evidenced by the results of the micro-CT and fluorescence analyses. The percentage of vertical height in the PV-nHA group was higher than in the other three groups at two time points (0.75%±0.53% at 4 weeks and 0.83%±0.42% at 6 weeks). Both rhVEGF$_{165}$ and cortical perforation could improve angiogenesis and osteoinduction in the central area of nHA blocks, increasing vertical bone regeneration. VEGF and decoration might function synergistically to improve vertical bone regeneration. We provide some insights into the clinical applications of nHA blocks.

Introduction

Bone graft substitutes, barrier membranes, autogenous bone tissue and the combined application of growth factors have been widely used as techniques to improve bone regeneration as treatments for bone infection or bone insufficiency caused by trauma, severe periodontitis, bone tumors, tooth extraction or the long-term use and removal of partial dentures.[1–4] The loss of bone tissue often results in complex horizontal and vertical alveolar ridge defects.[3] Therefore, an ideal bone substitute is considered one with good osteoconductivity and osteoinductivity for better bone regeneration, particularly for vertical augmentation. Autogenous bone grafts have been considered and applied as the gold standard for treating alveolar bone defects and achieving bone regeneration,[6] due to their high osteoconductive and osteogenic capacity and lack of immunogenicity and risk of causing disease.[4–6] However, the disadvantages of autogenous bone grafts, such as the need for a second surgery, tendency toward resorption (up to 60%),[7] insufficient amount of bone tissue, postoperative complaints and unpredictable results, may restrict their usefulness. Allografts and xenografts might be optimal bone substitutes, as they possess osteoconductive and osteogenic properties. However, the lack of osteoinduction, potential for infection, ethical issues and risk of immunological rejection remain unsolved problems. Onlay block grafting used to increase the height of the mandible or maxilla often requires fixation with screws and an autologous bone block from a donor site.[1] Sinus lifting is a commonly used procedure to increase the vertical bone volume, but this method is costly and complicated.[8] According to multiple studies, bone substitutes are potentially effective treatments for horizontal augmentation, but not for vertical augmentation.[9,10] The negative features of vertical augmentation are the lack of sufficient osseous bone walls and blood supplies, difficult fixation, large alveolar bone defects, insufficient osteoinduction and costly and complicated procedures (sinus lifting). Vertical augmentation is challenging and biologically demanding in dental implantology. In addition, angiogenesis originates from a certain distance within existing bone tissue, and the soft tissue must provide a stable environment for the increased dimensions of new bone formation. Although numerous therapies have been widely investigated to improve vertical bone augmentation, the most effective technique remains has not been clearly identified.[14–16] Bone grafts in the shape of blocks were introduced in the early 1990s to increase vertical bone regeneration in the maxilla and mandible. According to previous studies, a block-type bone substitute is beneficial for horizontal bone augmentation.[11] It has been proven to maintain sufficient amount of space, facilitate the operation and exhibit a good osteoconductive capacity, allowing the bone volume to be rebuilt.[12] However, as shown in the study by Kosaku Sawada,[5] the formation of a sufficient amount of new bone is not obtained when bone block substitutes are applied for more than 12 months for vertical bone augmentation. Several studies[12] have reported lower levels of vascularization in the central area of blocks and a low osteoinductive capacity in critical-size defects. These remaining problems restrict the clinical application of these materials in vertical guided bone augmentation or the treatment of critical-size or even larger bone defects. A limited number of studies have focused on the roles of vascularization and osteoinduction in the application of bone blocks. Guided bone regeneration (GBR) is based on the following four principles: epithelial and connective tissue exclusion, space maintenance, blood clot stability, and primary wound closure.[13,14] Four weeks after initiating GBR, new bone regeneration is possible when blood vessels are available. Regarding the healing process in GBR, the capability of bone graft substitutes to promote vascularization and osteoinduction is a key factor.[15,16] Angiogenesis is a multistep process and usually proceeds from existing blood vessels.[17,18] Therefore, improvements in the vascularization and osteoinduction of substantial block grafts remain a challenge in animal studies and clinical applications.

Cortical perforation, also called bone "decortication", "intramarrow penetration", and "marrow penetration", has

been used as part of the GBR procedure with or without barriers for attaining horizontal and/or vertical augmentation beyond the skeletal bone.[6,8,19–22] Penetration of the cortical bone into the cancellous bone with burs is recommended to improve bleeding and induce greater progenitor cell migration[29] into and blood vessel formation in the bone block substitutes.[23] In the study by De Carvalho,[24] autogenous cortical bone grafts placed on the mandible produced better healing at sites of decortication than at sites with no preparation. Toomo[25] reported the effectiveness of periosteal distraction with decorticating holes in new bone augmentation in rabbits, with an average result of 25.7± 5.1 mm^2 in the decoration group and 12.9 ± 3.2 mm^2 in the control group. However, the process of cortical perforation has not been supported in human clinical trials due to conflicting results and negative consequences in some animal studies,[26,27] including an increased operation time, additional bone loss, weakness at the receipt site and greater postoperative pain. Rasmusson[28] confirmed that GBR regenerates bone around exposed implant threads without decortication in a rat model. Data from clinical trials also revealed nonsignificant improvements in bone regeneration at 3 months after decortication in a rabbit animal model (75.5% versus 71.2%).[27] The literature does not seem to provide a clear answer regarding whether the application of cortical perforation improves or accelerates the process of bone regeneration. One possible reason might be the lack of an appropriate animal model to test the effect of cortical perforation on guided bone augmentation.

Hydroxyapatite (HA), a bone graft substitute, consists of a converted outer HA layer and an inner coralline core.[29] The physical properties of the mesoporous nanocomposite at the outer surface of HA enables drugs or proteins to be loaded in the scaffold.[30,31] Different shapes and size of HA have attracted increasing interest as a material to repair horizontal or vertical bone defect. Although HA has been proven to display excellent biocompatibility for osseous encapsulation in tissue engineering, the application of HA alone does not rapidly and efficiently induce the formation of new bone tissue.[29,32] In other reports, insufficient bone formation was observed in the central area of HA blocks due to lower levels of osteoinduction and vascularization during early healing.[12] The addition of growth factors (bone morphogenetic protein, BMP; human vascular endothelial growth factor, VEGF) might promote the osteoinductive capacity and improve bone augmentation. VEGF, a growth factor well known for inducing the migration, proliferation, and differentiation of vascular endothelial cells, has the capacity to upregulate the expression of BMP-2 and enhance new vessel formation and bone formation.[33] VEGF delivery increases bone regeneration by promoting neovascularization, bone turnover, osteoblast migration, and mineralization.[34] In our previous study, we evaluated the effect of nHA blocks coated with recombinant human vascular endothelial growth factor165 ($rhVEGF_{165}$) via physical adsorption on healing in a dog model of a critical size bone defect in the mandible and observed that angiogenesis in the nHA blocks improved horizontal bone regeneration, during the early stage of healing at 3 weeks.[12] These results prompted us to investigate whether localized VEGF delivery to bone blocks might be a viable strategy to accelerate bone healing and improve vertical bone regeneration. We hypothesize that the combination of cortical perforation and $rhVEGF_{165}$ might exert a synergistic effect on improving the osteoinductive capacity of nHA blocks and results in better vertical augmentation.

The aims of this study were to confirm that cortical perforation of the recipient bed is necessary and to evaluate whether the combined application of porous nHA block grafts coated with $rhVEGF_{165}$ and cortical perforation in a rabbit calvarial defect model synergistically improves vertical guided new bone regeneration.

Materials and Methods

Characteristics of the Material and Soak-Loading of $rhVEGF_{165}$

Twenty-four cylindrical nHA blocks (diameter, 5 mm; height, 3 mm) were supplied by Beijing YHJ Science and Trade Co., Ltd. (Beijing, People's Republic of China). According to our previous study, all blocks were sterilized with 25 kGy of γ radiation before the animal experiments. The ultrastructure of the nHA blocks was evaluated by a solution containing 12 μg/mL[12,35] using a scanning electron microscope (SEM, JSM-6300, JEOL Co., Ltd., Tokyo, Japan) at 20 kV. For soak loading, the nHA blocks were prepared and incubated with $rhVEGF_{165}$ (PeproTech Co., Ltd., USA) using a negative-pressure and adsorption method, as described in our previous study.[12] Each sample incubated with 0.02 mL the 12 μg/mL $rhVEGF_{165}$ solution (0.27 μg of $rhVEGF_{165}$ per block) was implanted within 30 minutes and then stored at −20°C until use.

Experimental Animals

Twelve male New Zealand rabbits (2.5–3.0 kg) were used in this study. The animals were housed in separate cages and kept under standard conditions. The preparation protocol was approved by the Committee for Animal Research (Guangdong, China). The animal procedures were conducted in accordance with guidelines for the management and use of laboratory animals provided by the Guangdong Provincial Medical Experimental Animal Center.

Assignment to Experimental Groups

Each animal was randomly assigned to the following four experimental groups, according to the surgical protocol, which included the use of titanium domes (Figure 1A–C):

(1) N-nHA group: nHA block on a nonperforated recipient bed,

(2) NV-nHA group: nHA block coated with $rhVEGF_{165}$ on a nonperforated bed,

(3) P-nHA group: nHA block on a perforated recipient bed, and

(4) PV-nHA group: nHA block coated with $rhVEGF_{165}$ on a perforated bed.

Surgical Procedure

The animals were anesthetized with an intramuscular injection of a mixture of ketamine hydrochloride and xylazine (Rompun, Bayer Korea, Seoul, Korea). The surgical site was shaved and then disinfected with an iodine tincture (2% lidocaine; lidocaine HCl, Huons, Seoul, Korea). An incision was made through the midline of the frontal bone to the occipital bone, and a full-thickness flap was prepared to expose the surgical area. Four standardized circular grooves were prepared using a trephine (Stoma, Storzam Mark GmbH, Ltd., Emmingen-Liptingen, Germany). The cortical perforation of the recipient bed was generated using a round, 1.4-mm-diameter carbide bur. Blocks coated with or without $rhVEGF_{165}$ were randomly assigned to the grooves in the calvarium of rabbits in the groups listed above (Figure 2A–C). The titanium domes (Figure 1C, inner diameter, 6.0 mm; outer diameter, 7.0 mm; height, 5 mm; volume, 169.56 mm^3) were designed to exactly fit the grooves (Figure 2D). The decoration rate (DR, area of decoration/area of circular groove) in the P-nHA and PV-nHA groups was 21.78%. The skin and periosteal flaps were repositioned and closed using nonabsorbable sutures (Jinghuan, 4–0, Gold Medical Supplies Co., Ltd., Shanghai, China). All animals received an intramuscular injection of benzyl penicillin (Longteng Pharmaceutical Company, Sichuan, China) at a dose of 2.5×10^4 U/kg for 3 days after the operation. As a fluorochrome bone label, tetracycline (MdBio Biotech Co., Ltd., Qingdao, Shandong, China) was administered at a dose of 25 mg/kg on the 13th and 14th days before euthanasia, and 5 mg/kg calcein (SIGMA, Sigma-Aldrich, St. Louis, MO, USA) was administered on the 3rd and 4th days before euthanasia.

Specimen Preparation

Experimental animals were sacrificed by an overdose of anesthesia at 4 and 6 weeks after surgery (Figure 2E and F). The harvested block sections, including the titanium dome, the host recipient bone bed and the graft, were dissected and fixed with 10% neutral-buffered formalin for 10 days.

Radiographic Evaluation

Prior to sectioning and the histological analysis, the fixed block specimens (the whole rabbit skull with the 4 different samples) were scanned using micro-computed tomography (micro-CT, ZKKS—MCT—Sharp—I, Caskaishen, China) at a resolution of 35 mm (60 kV and 40 W). The scanned data sets were processed and saved in DICOM format. The areas of interest were reconstructed using OnDemand three-dimensional (3D) software (MedProject) for a more in-depth investigation. The host bone and titanium dome were selected as a region of interest (ROI). The ratio of

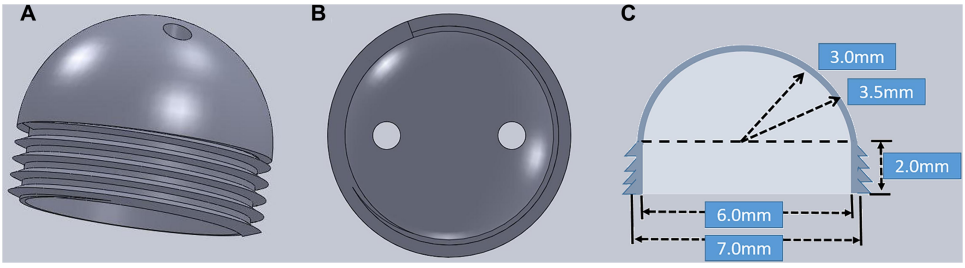

Figure 1 The nonabsorbable titanium dome of hemispheric shape: (**A**) the side view; (**B**) the top view; and (**C**) a thickness of 0.5 mm, an inner radius of 3.0 mm, an outsider radius of 3.5 mm and a screw height of 2.0 mm.

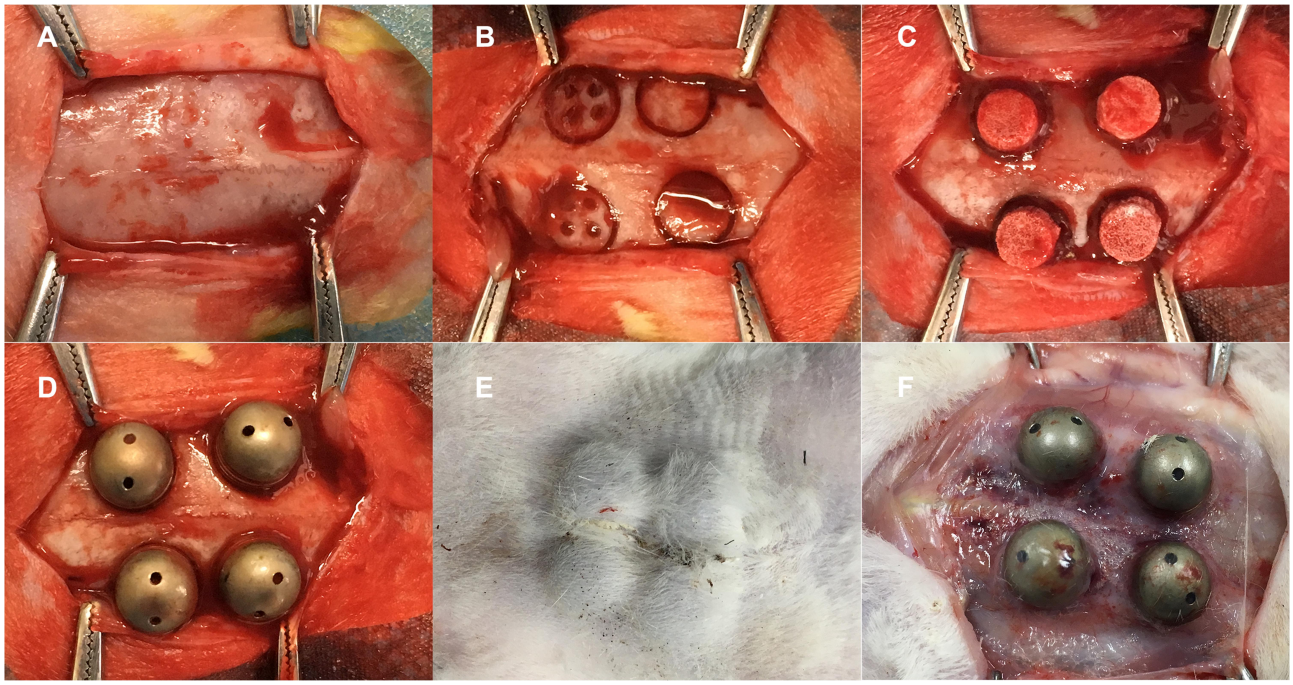

Figure 2 A depiction of the surgical procedure. (**A**) An incision was made through the midline of the frontal bone on the rabbit skull. (**B**) Four standardized circular grooves were generated by a trepan borer with an inside diameter of 6.0 mm and outer diameter of 7.0 mm, cortical perforations were generated with a 1.4-mm-diameter carbide round bur. (**C**) The bone blocks were placed in the circular grooves. (**D**) The titanium domes covered the bone blocks. (**E**) General view of the rabbit skull after 4 or 6 weeks of healing. (**F**) The four titanium domes were fixed tightly after 4 or 6 weeks healing.

the newly formed bone volume to the titanium dome volume (BV/TV) and the newly formed bone mineral density (BMD) in this region were analyzed at 4 and 6 weeks.

Histological and Fluorescence Microscopy Analyses

The histological and radiographic analyses were performed and analyzed by the same experienced researcher. The harvested block sections with the titanium domes were dehydrated in ascending concentrations of ethanol (70%, 80%, 95%, and 100%). The biopsies were infiltrated with methyl methacrylate (MMA, Sinopharm Chemical Reagent Co., Ltd., Shanghai, China) and stored in the refrigerator at 48°C for 3 days.[36] The undecalcified biopsies were pruned to histological sections with an approximate thickness of 100 μm using a microtome (EXAKT 300 CP, Germany). Each section with two domes was ground to a thickness of 50–60 μm using an automatic grinder (EXAKT400CS, Germany). All specimens were analyzed with a fluorescence microscope (Leica SP8 Laser Scanning Confocal Microscope, Germany). Photomultiplier filters (wavelength, 460–495 nm) were used to observe calcein and tetracycline, as described in our previous study.[36] An automated image analysis system (Leica Application Suite X, Microsystem, Germany) was used for the analysis, and the data were measured and collected as follows:

1. Percent area filled with new bone (NB %): the area filled with new bone (including the nHA block)/the whole area of the inner titanium dome on the coronal plane.
2. Percent vertical height of new bone tissue (VH %): the VH of new bone tissue/the middle height of the titanium dome on the coronal plane.
3. Percent of new bone dome contact (BDC %): the percentage of new trabecular bone in contact with the inner surface of the dome on the coronal plane.

Statistical Analysis

Outcome parameters obtained from the micro-CT and histomorphometric fluorescence analyses were calculated and summarized as the means and standard deviations. Statistically significant differences were determined using one-way ANOVA. Multiple groups were compared with a post-hoc test using the statistical software program SPSS ver. 17.0 (SPSS, Inc., Chicago, IL, USA) with a critical value of $[\alpha] = 0.05$.

Results

Characterization and Topography of the Material

Images were captured at magnifications of 26, 5000 and 50,000 (Figure 3A–C). Figure 3 shows SEM photomicrographs of the nanoporous network structure on the surface of the nHA blocks. The 3D macroporous structure of the blocks consisted of multiple and diverse pores. Furthermore, these macrospores were suitable for cell attachment and proliferation or angiogenesis. The nanoscale crystals of the nHA are clearly observed in the high-magnification SEM images (Figure 3C). The interconnected pores with diameters of 107–550 μm and the nanoscale HA pores with diameters of 71–99 nm were consistent with the findings of our previous study.[12]

Clinical Outcomes

No rabbits were lost during the procedure or the follow-up period. All of the titanium domes were anchored to the rabbit calvarium, and no complications, including wound dehiscence, severe swelling, and bleeding, were observed during the subsequent 4 or 6 weeks.

Micro-CT Evaluation

Based on the micro-CT images, a dome-shaped space between the host cortical bone line and the titanium dome was formed by the bone block and new bone tissue. The integrated nHA block graft and the new trabecular tissue were clearly observed in all groups at 4 (Figure 4A–D) and at 6 weeks (Figure 5A–D). Horizontal and cross-sectional micro-CT images were obtained. The nHA block was marked in gray. The host bone of the rabbit skull was marked in yellow. The new bone tissue was marked in green. Notably, new bone tissue was present at the center and the periphery of the nHA blocks, particularly in the PV-nHA group, at 4 (Figure 4D) and 6 weeks (Figure 5D). Minimal resorption of the host cortical bone or the bone block was observed, but the original shape was maintained at both time points. A greater volume of new trabecular tissue was observed in the vertical central area of the PV-nHA group at 4 and 6 weeks than in the other three groups. The BV/TV and BMD were higher at 6 weeks than at 4 weeks (Table 1). Significantly higher values of the two parameters were recorded for the PV-nHA group than the N-nHA group ($P<0.05$) at 4 and 6 weeks. The mean BV/TV was 67.82 ±1.93% in the P-nHA group and 62.64±4.72% in the N-nHA group at 6 weeks, and the difference was statistically significant. The mean BMD at 4 weeks was 955.46±59.8 g/cc and 924.11±22.9 g/cc in the P-nHA and N-nHA groups, respectively, and the differences were statistically significant.

Histological and Fluorescence Microscopy Analyses

Each histological section from the four groups (N-nHA, NV-nHA, P-nHA and PV-nHA groups) were clearly observed at the two time points (Figures 6 and 7). The titanium dome-shaped space remained and was clearly observed after a series of nondecalcification procedures. The tetracycline fluorochrome bone label appeared bright green, and calcein appeared orange-yellow.

In all groups, the newly formed trabecular bone tissues with different vertical heights were integrated with the nHA blocks at 4 and 6 weeks. Both the new bone tissue and the blocks were clearly distinguished from the basic line of the rabbit skull.

At 4 weeks, the nHA blocks exhibited rare resorption along the coronal plane, but these areas were located at the periphery of the dome-shaped space, where no fixation occurred between the block and the host bone bed. Blank areas were still observed at the top of the dome-shaped area. Multiple new trabecular bone penetrations were observed in

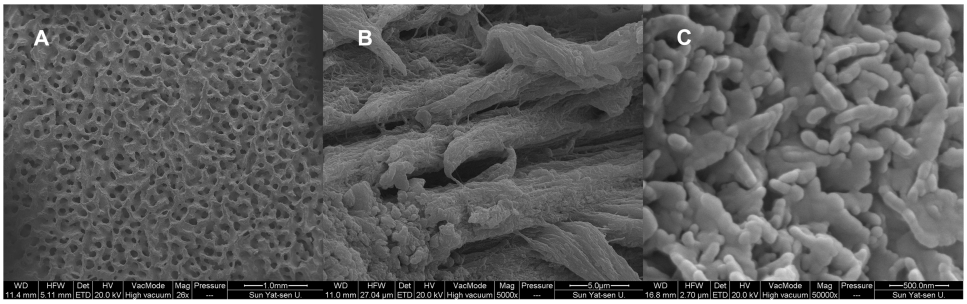

Figure 3 (**A**) SEM micrographs of the porous n-HA block surface with multilevel pores, 26×, bar = 1 mm. (**B**) Images of the micro pits resulting from the visualized block surface, 5000×, bar = 5 μm. (**C**) High-magnification SEM images of nano-scale, 50,000×, bar = 5 nm.

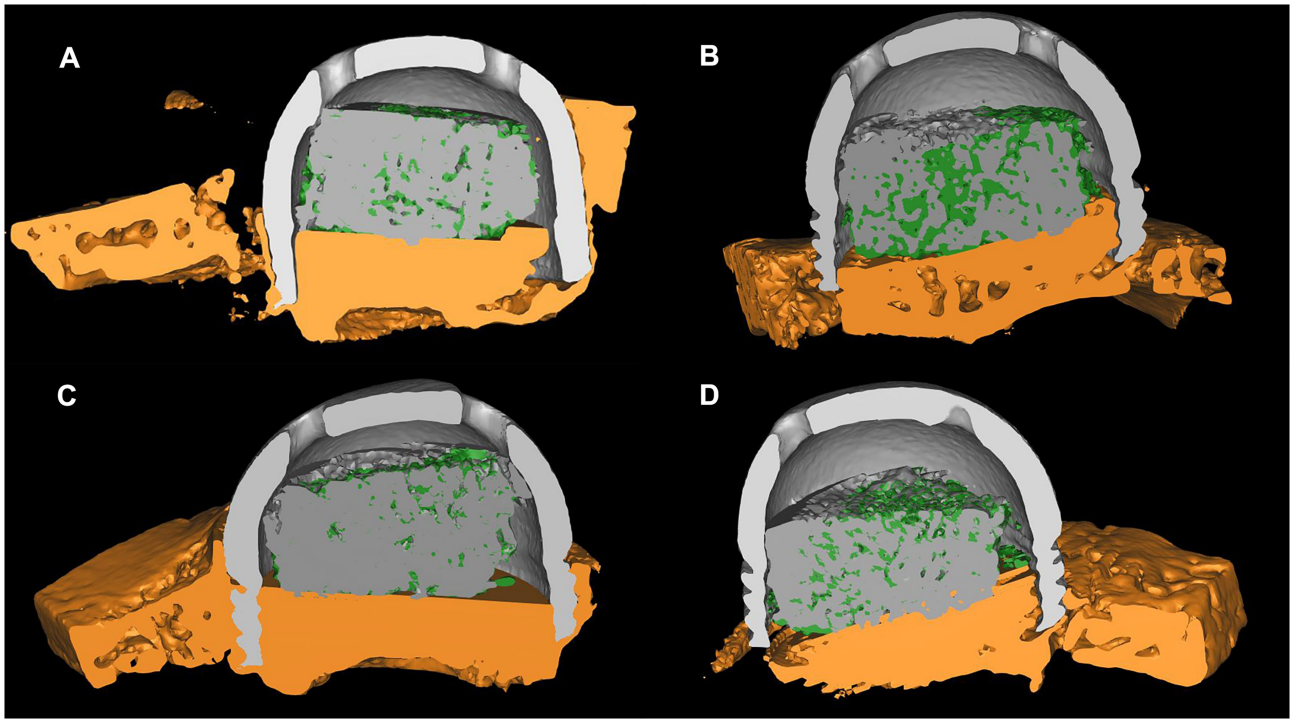

Figure 4 Reconstructed micro-CT images of the four different groups at 4 weeks after surgery.
Notes: (**A**) N-nHA, (**B**) NV-nHA, (**C**) P-nHA, and (**D**) PV-nHA. (The titanium dome is marked with a light gray color. The nHA bone block is showed in grey. The host bone of the rabbit skull is showed in yellow. The new bone tissue is showed in green.)

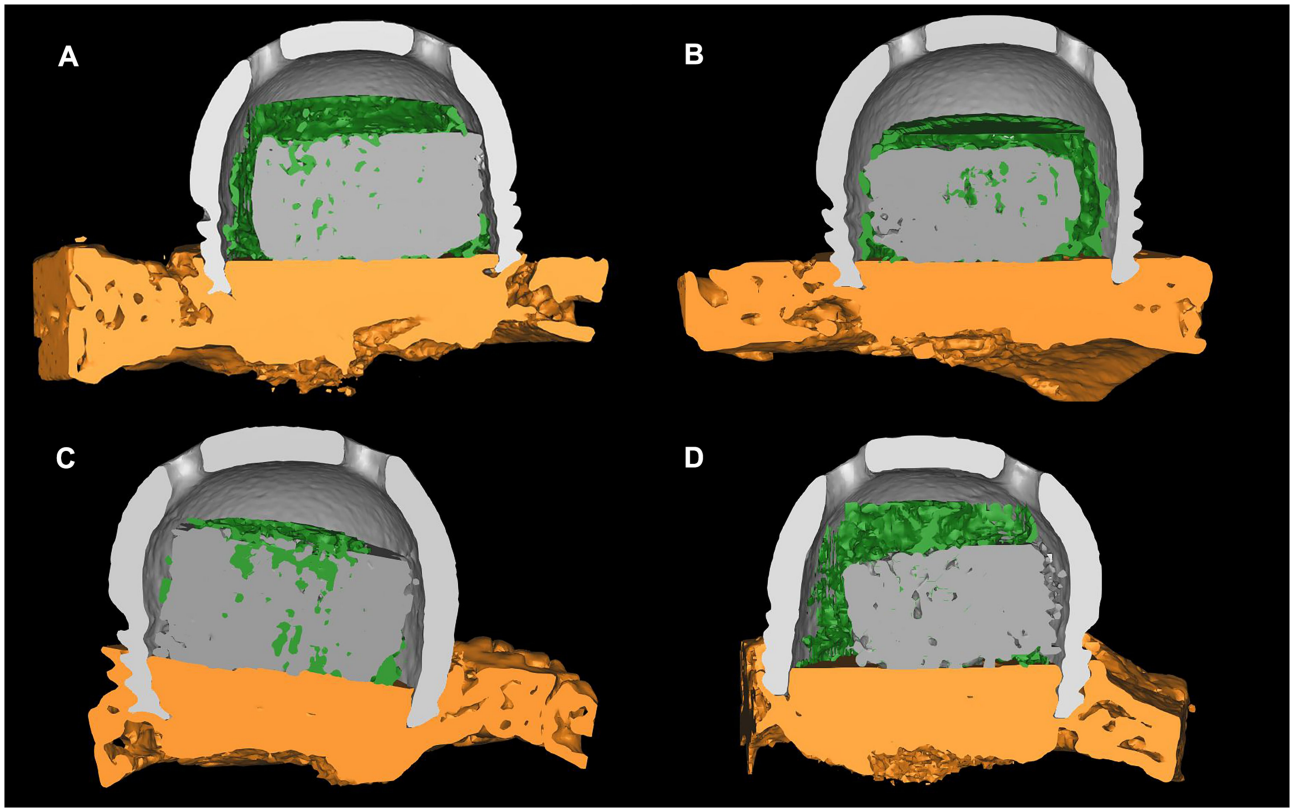

Figure 5 Reconstructed micro-CT images of the four different groups at 6 weeks after surgery.
Notes: (**A**) N-nHA, (**B**) NV-nHA, (**C**) P-nHA, and (**D**) PV-nHA. (The titanium dome is marked with light gray color. The nHA bone block is showed in grey. The host bone of the rabbit skull is showed in yellow. The new bone tissue is showed in green.)

Table 1 Descriptive Statistics for the BV/TV and BMD (Micro-CT) Analysis by Group and Endpoint

Outcome	Endpoint	Parameter	Group			
			N-nHA	NV-nHA	P-nHA	PV-nHA
BV/TV(%)	4 weeks	n Mean±SD 95% CI	6 58.26±4.4◆ 53.62–62.91	6 62.15±5.06 56.84–67.46	6 62.32±5.98 56.05–68.60	6 66.32±4.35◆** 61.76–70.89
	6 weeks	n Mean±SD 95% CI	6 62.64±4.72◤★ 57.68–67.60	6 66.25±2.83□ 63.28–69.22	6 67.82±1.93◤** 65.80–69.84	6 70.79±3.09★**□ 67.55–74.03
BMD(g/cc)	4 weeks	n Mean±SD 95% CI	6 924.11±22.9•** 900.04–948.19	6 928.31±37.7▲** 888.67–967.95	6 955.46±59.8■** 892.65–1018.28	6 1049.04±51.92•▲■ 994.55–1103.53
	6 weeks	n Mean±SD 95% CI	6 987.60±50.9◢** 934.16–1041.04	6 1015.75±62.45○ 950.21–1081.29	6 1033.00±24.64 1007.15–1058.87	6 1078.04±62.6◢○ 1003.55–1053.65

Notes: ◆◤★□•▲■◢○$P<0.05$, and **$P<0.01$.

Abbreviations: BV, new bone volume; TV, total volume; BMD, bone mineral density; SD, standard deviation; 95% CI, 95% confidence interval for mean.

the blocks and along the inner surface of the titanium domes, particularly in the PV-nHA group (Figure 6D). The interface between the bone block and the host bone appeared as a continuous line in the groups without cortical perforation, ie, the N-nHA (Figure 6A) and NV-nHA (Figure 6B) groups. However, bony bridge integration with intense fluorescence was obviously present in the areas of cortical perforation in the P-nHA (Figure 6C) and PV-nHA groups (Figure 6D). The outer surface of the blocks in the groups with cortical perforation or blocks coated with rhVEGF$_{165}$ appeared to contain numerous blood vessels, which enhanced woven bone formation. The histological and fluorescence microscopy analyses revealed a mean NB% of 0.54±0.95% in the N-nHA group, 0.59±0.84% in the NV-nHA group, 0.60

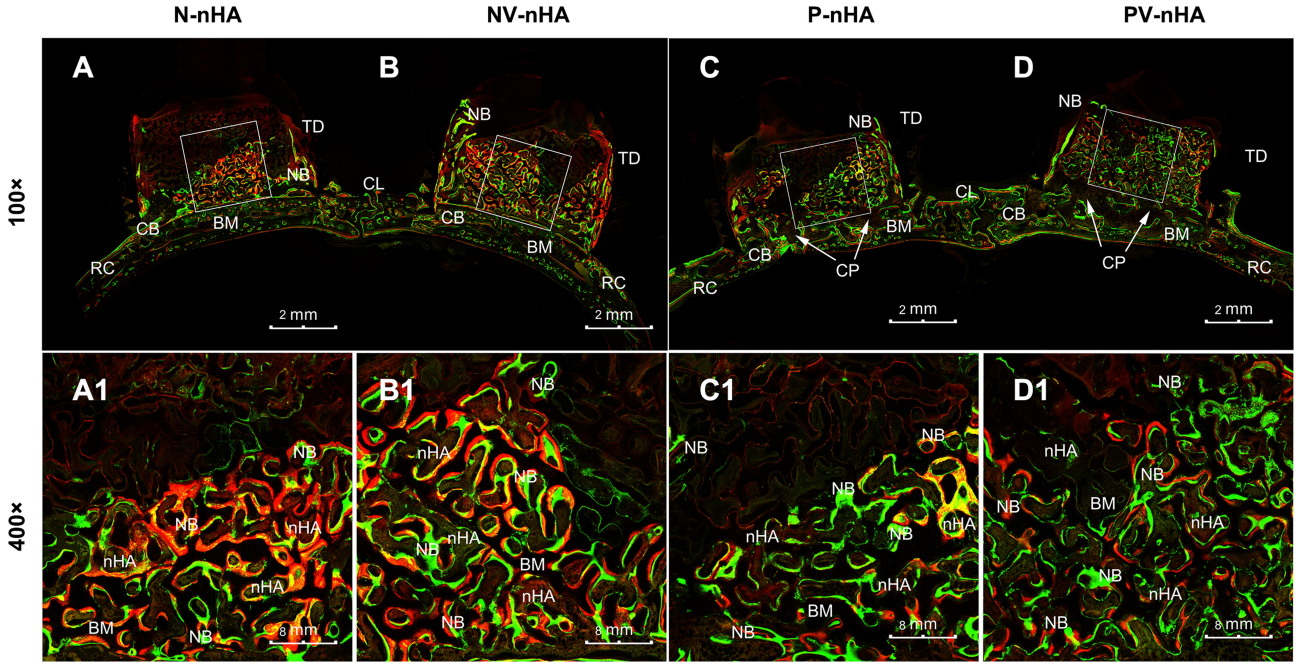

Figure 6 Fluorescence images of coronal sections of the rabbit calvarium at 4 weeks after implantation: (**A**) N-nHA group, (**B**) NV-nHA group, (**C**) P-nHA group, and (**D**) PV-nHA group. The trabecular bone, cortical perforation, dome, rabbit calvarium and midline are indicated in the images.

Abbreviations: NB, new bone; nHA, nano-hydroxyapatite block; BM, bone marrow; CP, cortical perforation; TD, titanium dome; CL, central line; RC, rabbit calvarium.

±0.68% in the P-nHA group and 0.75±0.59% in the PV-nHA group. The differences between the PV-nHA group and the other three groups were statistically significant (Figure 8A). Compared with the N-nHA group (0.575±0.10%) and the NV-nHA group (0.65±0.10%), the VH% in the PV-nHA group (0.75±0.53%) was significantly larger at 4 weeks (Figure 8B). Moreover, the inner surface of the domes was filled and connected with slender bone trabeculae. The highest BDC% was observed in the PV-nHA group (0.61±0.96%) compared with the other three groups, and the value was significantly higher than that in the N-nHA group (Figure 8C).

The VH% of new bone tissue in all groups (Figure 7A–D) was greater at 6 weeks than at 4 weeks. The bone trabeculae, which were dark green and yellow-green in color, became more slender and more elongated (Figure 7A1–D1). The titanium dome-shaped space, the periphery adjacent to the host bone and the center of the nHA block were completely filled with slender, elongated and interconnected trabeculae. Interestingly, in the P-nHA group (Figure 7C) and the PV-nHA group (Figure 7D), new bone tissue formed beyond the original upper margin of the nHA block, up to the top of the dome. The NB% was 0.63±0.03% in the N-nHA group, 0.70±0.37% in the NV-nHA group, 0.76±0.10% in the P-nHA group and 0.81 ±0.47% in the PV-nHA group. The differences between the groups (PV-nHA vs N-nHA, PV-nHA vs NV-nHA, and P-nHA vs N-nHA) were statistically significant

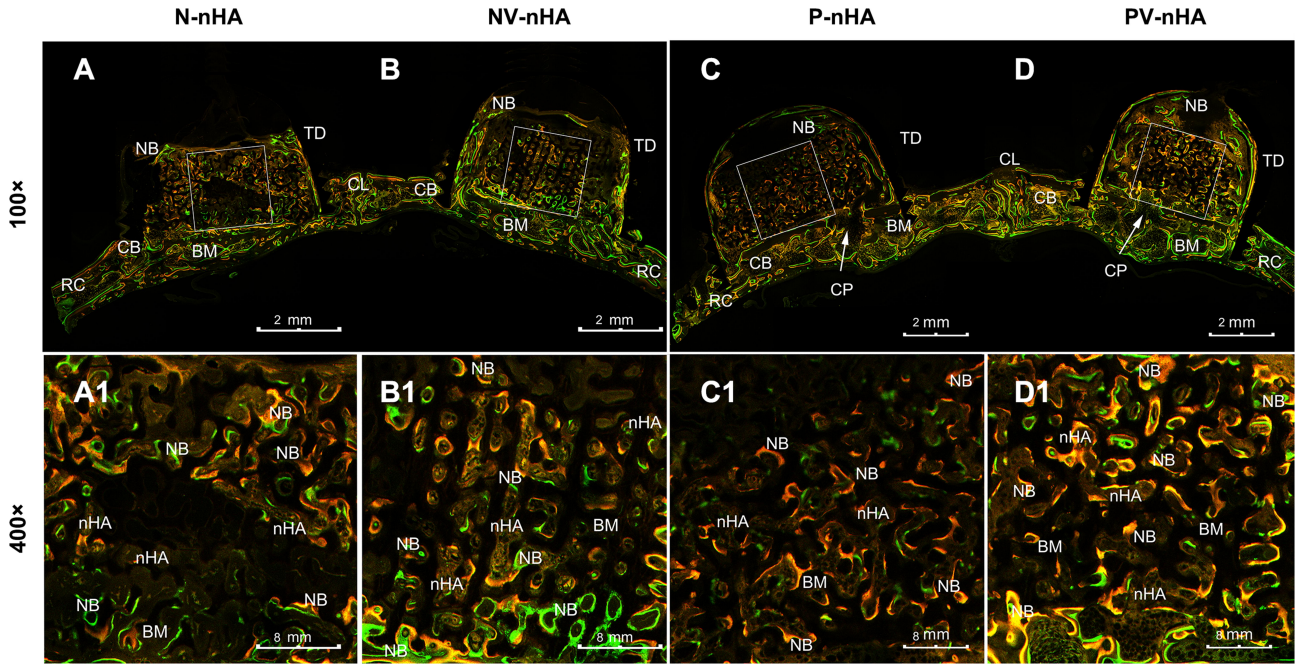

Figure 7 Fluorescence images of coronal sections of the rabbit calvarium at 6 weeks after implantation: (**A**) N-nHA group, (**B**) NV-nHA group, (**C**) P-nHA group, and (**D**) PV-nHA group. The trabecular bone, cortical perforation, dome, rabbit calvarium and midline is indicated in the images.
Abbreviations: NB, new bone; nHA, nano-hydroxyapatite block; BM, bone marrow; CP, cortical perforation; TD, titanium dome; CL, central line; RC, rabbit calvarium.

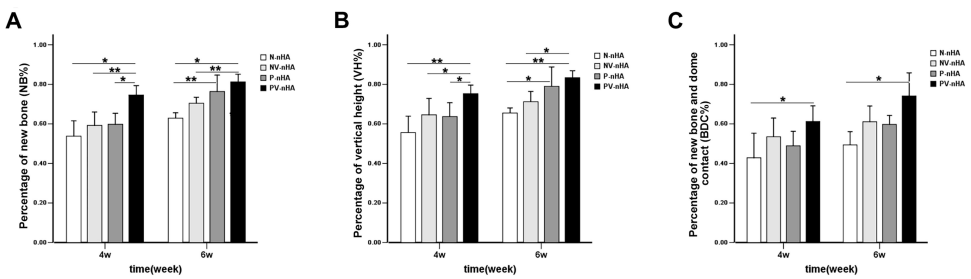

Figure 8 Results of the statistical analysis of the newly formed bone in fluorescence images of coronal sections. The differences of NB% (**A**), VH% (**B**) and BDC% (**C**) were quantified (n=6).
Notes: *P<0.05, and **P<0.01.

(Figure 8A). A noticeably greater VH% was recorded for the PV-nHA group (0.83±0.42%) than in the other two groups (0.66±0.32% for the N-nHA group; 0.71±0.64% for the NV-nHA group), and the differences were significant (Figure 8B). The BDC% in each group was greater at 6 weeks than at 4 weeks. The difference in the BDC% between the PV-nHA group (0.74±0.14%) and the NV-nHA group (0.49±0.82%) was statistically significant (Figure 8C).

Discussion

Vertical guided bone regeneration was clearly achieved using porous nHA block grafts coated with rhVEGF$_{165}$ and cortical perforation of the recipient bed in this study, as determined by micro-CT and histological fluorescence analyses. The figures and data showed that nHA blocks coated with rhVEGF$_{165}$ successfully integrated with the perforated cortical bed in a rabbit calvarial defect model. Animal models for studying horizontal augmentation have been well established and documented, with low complication rates. However, establishing an animal model for studying vertical bone augmentation in human mandible has remained a challenge.[37,38] An appropriate model and research protocol must be chosen to effectively analyze the effects of bone substitute materials.[39] Bone augmentation procedures must ensure the mechanical stability of bone substitute materials, avoid fibrous tissue encapsulation and promote bone regeneration.[9,40] In our study, a titanium dome with self-tapping screws was designed to achieve good retention. The interfaces between the titanium dome, host bone, and block grafts in the different groups were compared. This optimal rabbit calvarial defect model is recommended for studies evaluating vertical guided bone regeneration due to its resemblance to the human mandible, with a poor blood supply and limited bone marrow.[36] In the present study, we evaluated the outcomes of nHA block grafting without rigid fixation at 4 and 6 weeks postoperatively, representing the early and late phases of healing. This animal model provided an obvious line to distinguish the baseline with or without cortical perforation, the vertical height of newly formed bone tissue, the borderline between the nHA block and new trabecular bone and the amount of bone regeneration. Fluorescein labeling for new bone regeneration is considered an effective method to visualize new trabecular bone tissue.[36] When different fluorochromes are injected into experimental animals at different points during the ossification process, they bind to the available calcium and precipitate in the mineralized bone tissue.[41] In our previous studies, calcein and oxytetracycline were used for fluorescein labeling to obtain high-quality images of mineralized bone tissue in vivo using epifluorescence microscopy.[36] The fluorescence analysis might be not sufficiently thorough to represent all changes inside the titanium dome. A micro-CT analysis[20] has been recommended to measure the mineralized bone tissue in a GBR animal model due to its high precision and capability for spatial reconstruction (1 to 3 μm for micro-CT and 300 μm for cone-beam CT). Go Kochi[42] used micro-CT and histomorphometry to observe bone augmentation in the rat calvarium. 3D micro-CT was planned to observe the healing pattern of the nHA blocks and the total newly bone volume.

HA, with a general formula of $Ca_{10}(OH)_2(PO_4)_6$, is chemically similar to the inorganic component of the bone matrix. Regarding the interconnected pores and pore size of bone substitutes, numerous studies[43] have revealed that the properties of HA with nanostructures improve cell attachment and bone regeneration in alveolar bone defects. According to Dorozhkin,[11] recent developments in various nanoscale and nanocrystalline bone substitutes affect the biological activities in terms of synthesis and characterization as well as biomedical and clinical applications. Ben-Nissan[43] applied an HA nanocoating to a micro/nano porous bone substitute material for application as a load-bearing bone graft with specific strength requirements. The SEM images (Figure 3C) obtained in the present study revealed that a pore size of nHA blocks ranging from 107 to 550 μm, with nanoscale features ranging from 71 to 99 nm. The results were consistent with previous studies,[12] which suggested that the application of nHA blocks is beneficial for horizontal or vertical augmentation.

Recently, the application of bone substitutes for critical-size defects in alveolar bone has been studied and yielded good results in animal models. However, vertical regeneration of the alveolar ridge remains a challenge and a key problem in dental implantology.[9,10] Angiogenesis is a critical step required prior to bone formation. As one of several methods to improve the blood supply and promote angiogenesis, cortical perforation has been applied to the recipient bed without creating a donor site.[44] In previous clinical studies and case reports, cortical perforation has been recommended as a part of the GBR protocol to improve bone regeneration. However, researchers have questioned whether cortical perforation of the recipient bed is necessary to attain extraskeletal vertical bone

augmentation. Both the rabbit calvarium and human mandible originate from intramembranous bone and have the physiological characteristics of a low marrow content and limited vascular supply.[1] Therefore, we performed cortical perforation in our animal experiment to examine whether it increases the amounts of blood, oxygen, and nutrients supplied by the host bone for vertical bone formation. Histological and fluorescence analyses, showed multiple bone trabeculae penetrating the nHA block from the areas of original calvarial bone with cortical perforation at 4 weeks, during the early stage of healing. Thus, cortical perforation should be considered as a regional acceleratory phenomenon.[45] The vascularity peaked after the application of a noxious stimulus to cortical bone and decreased to normal levels after healing. Moreover, drilling holes through cortical bone into vascular cancellous bone led to bleeding and clot organization, which induced the release of cytokines and growth factors to attract more progenitor cells and osteoblasts. The fluorescence analysis revealed statistically significant differences in the NB% and VH% between the groups with and without cortical perforation (PV-nHA group compared with the NV-nHA group) at 4 and 6 weeks. In addition, the BV/TV in the P-nHA group was significantly greater than the value in the N-nHA group (67.82±1.93% compared with 62.64 ±4.72%) at 6 weeks. Interestingly, the study by Norton and colleagues, similar amounts of newly formed bone and residual graft particles at sites augmented with cortical perforation were observed after a healing period of 26 weeks.[46] Danesh-Sani documented a significant increase in the number of new vessels in the test group with cortical bone perforation compared with the control group after a healing period of 7 months.[8] These findings further supported the hypothesis that cortical perforation provides passageways for blood vessels and progenitor cells to rapidly obtain access to a GBR site.

In tissue engineering, biological substitutes are often used to restore bone defects, maintain space and improve hard or soft tissue regeneration. According to the principles of both engineering and biology, this concept involves three main strategies: using cells or cell substitutes to replace limited tissue functions; improving the osteoinductivity of substitute materials, such as the application of growth factors; and designing biological scaffolds to support and direct tissue development.[47] In previous studies, nHA blocks with a slow degradation rate maintained their volume and provided space even in the late period. However, the healing capacity of nHA blocks was still inferior to autologous bone grafts, specifically in terms of initial osteoinduction, and progressive graft resorption.[48] According to Kosaku Sawada,[5] block substitutes show limited bone formation and material resorption, even after 12 months of healing. Taken together, bone block substitutes are not ideally suitable for vertical bone augmentation in the treatment of severe bone defects due to reduced contact with the host bone and limited vasculature. Consistent with the results described above, our fluorescence analysis (Figures 6A and A1 and 7A and A1) showed a low signal and height in the central areas compared with the side areas of the nHA blocks in the N-nHA group at 4 and 6 weeks, which indicated a low level of angiogenesis and bone regeneration. Nevertheless, the ability to maintain the volume of bone substitute while improving the capacity for neovascularization and osteoinduction for better vertical new bone regeneration remain key problems for dentists.

The use of mesenchymal stem cells or growth factors is recommended to promote angiogenesis and osteoinduction.[12,49] VEGF-A, a member of the VEGF family, has been identified as the main factor that promotes both physiological and pathological angiogenesis. At least five different molecular isoforms of VEGF (with 121, 145, 165, 189 and 206 amino acids, respectively) have been identified. $VEGF_{165}$ is considered the most predominant and potent molecule produced by a variety of normal and transformed cells. Seventy percent of $VEGF_{165}$, the most abundant isoform in humans, remains in the extracellular matrix. It is a potent mitogen for endothelial cells and plays a key role in normal and pathological angiogenesis.[50] The application of VEGF activates endothelial cells in the surrounding tissue by stimulating cell liberation, migration, and proliferation, and finally the formation of tubular structures.[51] As shown in the study by Mayr-Wohlfart,[34] VEGF-A might not only induce angiogenesis to facilitate bone formation but also stimulate the process in a direct manner by inducing the proliferation and migration of osteoblasts. Another study[52] provided strong evidence that VEGF functions as a survival factor for endothelial cells and immature vessels. In our previous study,[12] the nHA blocks coated with $rhVEGF_{165}$ via a direct physical adsorption approach promoted angiogenesis at 3 weeks in critical size mandibular bone defects in dogs, during the early stage of healing. The critical size bone defects with three walls in the mandible were a good model for assessing the effect on horizontal bone regeneration. However, the interference of blood vessels or osteoblasts from the three walls of the bone defects was

unable to be excluded. In addition, the application of porous nHA blocks provides more functional groups, such as –OH, $–NH_2$, and $–COOH^-$ groups.[29] These functional groups might facilitate direct adsorption and sustained release. Therefore, our study focused on the effect of VEGF on the central area of the blocks and on vertical augmentation in a rabbit calvarial defect model. The outcome measures of micro-CT and fluorescence microscopy, ie, the mean BV/TV%, NB%, VH% and BDC%, were obviously higher in the NV-nHA group than in the control (N-nHA) group, but the differences were not statistically significant (Table 1 and Figure 8).

Importantly, we hypothesized that the combination of nHA blocks coated with $rhVEGF_{165}$ and cortical perforation might exert a synergistically effect on improving vertical bone regeneration by directly affecting primary osteoblasts and promoting angiogenesis. According to previous studies, VEGF, particularly VEGF-A, is produced by most parenchymal cells and acts in a paracrine manner on adjacent endothelial cells to regulate VEGF receptor signaling and biology.[49] All VEGF-A isoforms are able to activate two different tyrosine kinase receptors: VEGF receptor 1 (VEGFR1/Flt-1) and VEGF receptor 2 (VEGFR2/KDR/Flk-1).[50,53] Receptor activation in endothelial cells induces phosphorylation and leads to the transduction of different signals promoting cellular activities, such as endothelial cell migration and proliferation, subsequently enhancing angiogenesis.[54] Therefore, the issue of increasing VEGF release from the host bone tissue must be seriously considered. Cortical perforation of the recipient bed may induce the recruitment of osteoblasts, which are considered an important source of VEGF. The experimental results from the present study provided additional evidence supporting this hypothesis. Statistically significant differences in the BV/TV% and BMD were observed between the N-nHA and PV-nHA groups, as determined using micro-CT. Fluorescence microscopy clearly showed trabecular bone connected with the inner surface of the titanium dome in the PV-nHA group, nearly reaching the top at 6 weeks (Figure 7D). The percentage of new bone regeneration and vertical height were obviously greater in the groups with the $rhVEGF_{165}$ coating than in the groups without the $rhVEGF_{165}$ coating at 4 and 6 weeks. Furthermore, the differences in the NB% and VH % between the PV-nHA group and the N-nHA group were statistically significant at 4 and 6 weeks (Figure 8). Additionally, the bone trabeculae, which were dark green and yellow-green in color, became model slender and more elongated. Thus, VEGF might participate in the formation of immature vessels during the early stage of healing. The rate of new trabecular bone formation was slower and the newly formed bone tissue was more mature at 6 weeks than at 4 weeks.

As mentioned above, the rabbit calvarium has a poor blood supply due to the anatomy distribution of different arteries. The artery supplying the parietal bone is the posterior branch of the middle meningeal artery, emanating from the maxillary artery. One major branch of the meningeal artery curves toward the sagittal suture of each parietal bone. The result is arterial blood flow toward the midline.[55] This anatomy results in better perfusion of the lateral portions of the nHA block than the medial portions. Insufficient blood perfusion leads to uneven nutrient and oxygen supplies for new bone formation.[1,55] In the present study, the objective of the experiment was to overcome these limitations. Although some studies[29,56] have suggested that three functional groups in nHA crystals (–OH, –NH and $–COOH^-$) interact with protein molecules to yield greater bone formation, the response in the N-nHA group, which was not treated with any other growth factors, appeared unsatisfactory. Therefore, both cortical perforation in medial areas of the recipient bed and the physical adsorption of $rhVEGF_{165}$ were applied to the PV-nHA group. The VH% at the midline was higher in the PV-nHA group than in the other three groups at the two time points during the healing process (0.75±0.53% at 4 weeks and 0.83±0.42% at 6 weeks). Potential explanation for the aforementioned outcomes are that cortical perforation can increase the blood supply required to recruit progenitor cells from the host bone in the central areas, while $rhVEGF_{165}$ can induce the migration, proliferation and differentiation of vascular endothelial cells. Both of these factors contributed to the accumulation of osteoblasts and improvement of vertical bone augmentation.

More interestingly, the BDC% in the lateral areas near the inner surface of the titanium dome was higher than in the central areas in the groups with cortical perforation (P-nHA and PV-nHA groups). These results are consistent with the outcomes of a previous study by Zeeshan Sheikh.[1] Several possible explanations were analyzed. First, the observation is consistent with the anatomical contouring of the rabbit calvarial bone along with differences in the blood supply between the lateral and medial areas.[21] Second, some differences between decoration and $rhVEGF_{165}$ in terms of the potential to promote guided bone augmentation were observed. Third, the inner surface

of the titanium dome might have the capacity to attract more osteoblasts for contact osteogenesis due to its good biocompatibility. Fourth, the differential expression of the freely diffusible VEGF isoform $VEGF_{121}$ produced by osteoblasts from the host bed might contribute to the formation of an angiogenic gradient within the bone,[54] allowing communication with endothelial cells located some distance from the surface of newly forming bone.

Conclusions

In the present study, the rabbit calvarial defect model was proven to be an effective model for evaluating vertical guided bone regeneration due to its resemblance to the human mandible, with a poor blood supply and limited bone marrow. Cortical perforation provided passageways for blood vessels and progenitor cells to rapidly obtain access to the defect. Therefore, pretreatment with cortical perforation before GBR is necessary and recommended for better bone augmentation. The VH% at the midline of the block was higher in the PV-nHA group than in the other three groups at both time points (0.75±0.53% at 4 weeks and 0.83±0.42% at 6 weeks). The use of porous nHA block grafts coated with $rhVEGF_{165}$ and cortical perforation improved angiogenesis and osteoinduction in the central area, increasing vertical bone regeneration in the rabbit calvarial defect model, as determined using micro-CT and histological fluorescence microscopy. These functional groups of nHA blocks, such as –OH, $–NH_2$, and $–COOH^-$, facilitated the direct adsorption and sustained release of $rhVEGF_{165}$ in the central area. VEGF-A was produced by most parenchymal cells after cortical perforation and acted in a paracrine manner on adjacent endothelial cells to regulate VEGF receptor signaling and biology. VEGF and cortical perforation might exert synergistically effects on improving vertical bone regeneration by nHA block grafts by directly affecting primary osteoblasts and promoting angiogenesis and osteoinduction. This study provides some potential insights into the clinical applications of bone blocks; however, the effect on vertical bone regeneration requires further studied, particularly the possible mechanisms underlying the relationship between vascularization and bone regeneration.

Acknowledgments

This study was supported by the School of Stomatology, Southern Medical University (People's Republic of China) and grants from the Natural Science Foundation of China (81170998), the Fund of Guangdong Province Medical Science Research (A2020517), the Fund of Guangdong Province Medical Science Research (2016A030310240) and the Fund of Foshan Science and Technology Research (2018AB002711).

Disclosure

The authors report no conflicts of interest related to this work.

References

1. Sheikh Z, Drager J, Zhang YL, Abdallah MN, Tamimi F, Barralet J. Controlling bone graft substitute microstructure to improve bone augmentation. *Adv Healthcare Mater*. 2016;5(13):1646–1655. doi:10.1002/adhm.201600052
2. Sousa V, Mardas N, Farias B, et al. A systematic review of implant outcomes in treated periodontitis patients. *Clin Oral Implants Res*. 2016;27(7):787–844. doi:10.1111/clr.12684
3. Galindo-Moreno P, de Buitrago JG, Padial-Molina M. Histopathological comparison of healing after maxillary sinus augmentation using xenograft mixed with autogenous bone versus allograft mixed with autogenous bone. *Clin Oral Implants Res*. 2018;29(2):192–201. doi:10.1111/clr.13098
4. Barone A, Covani U. Maxillary alveolar ridge reconstruction with nonvascularized autogenous block bone: clinical results. *J Oral Maxillofacial Surgery*. 2007;65(10):2039–2046. doi:10.1016/j.joms.2007.05.017
5. Sawada K, Nakahara K, Haga-Tsujimura M, et al. Comparison of three block bone substitutes for bone regeneration: long-term observation in the beagle dog. *Odontology*. 2018;106(4):398–407. doi:10.1007/s10266-018-0352-7
6. Oh KC, Cha JK, Kim CS, Choi SH, Chai JK, Jung UW. The influence of perforating the autogenous block bone and the recipient bed in dogs. Part I: a radiographic analysis. *Clin Oral Implants Res*. 2011;22(11):1298–1302. doi:10.1111/clr.13410
7. Johansson B, Grepe A, Wannfors K, Aberg P, Hirsch JM. Volumetry of simulated bone grafts in the edentulous maxilla by computed tomography: an experimental study. *Dentomaxillofacial Radiol*. 2001;30(3):153–156. doi:10.1038/sj.dmfr.4600600
8. Danesh-Sani SA, Tarnow D, Yip JK, Mojaver R. The influence of cortical bone perforation on guided bone regeneration in humans. *Int J Oral Maxillofac Surg*. 2016;46:2.
9. Tamimi F, Torres J, Gbureck U, et al. Craniofacial vertical bone augmentation: a comparison between 3D printed monolithic monetite blocks and autologous onlay grafts in the rabbit. *Biomaterials*. 2009;30(31):6318–6326. doi:10.1016/j.biomaterials.2009.07.049
10. Urban IA, Montero E. Effectiveness of vertical ridge augmentation interventions: A systematic review and meta-analysis. *J Clin Periodontol*. 2019;46(Suppl 21):319–339. doi:10.1111/jcpe.13061
11. Ebrahimi M, Botelho M. Biphasic calcium phosphates (BCP) of hydroxyapatite (HA) and tricalcium phosphate (TCP) as bone substitutes: importance of physicochemical characterizations in biomaterials studies. *Data Brief*. 2017;10:93–97. doi:10.1016/j.dib.2016.11.080
12. Du B, Liu W, Deng Y, et al. Angiogenesis and bone regeneration of porous nano-hydroxyapatite/coralline blocks coated with rhVEGF165 in critical-size alveolar bone defects in vivo. *Int J Nanomedicine*. 2015;10(default):2555–2565.
13. Urban IA, Monje A. Guided bone regeneration in alveolar bone reconstruction. *Oral Maxillofac Surg Clin North Am*. 2019;31(2):331–338. doi:10.1016/j.coms.2019.01.003

14. Wang HL, Boyapati L. "PASS" principles for predictable bone regeneration. *Implant Dent*. 2006;15(1):8–17. doi:10.1097/01.id.0000204762.39826.0f
15. Yang HS, Epple C, Haumer A, et al. Prefabrication of a large pedicled bone graft by engineering the germ for de novo vascularization and osteoinduction. *ACS Appl Mater Interfaces*. 2019;192:118–127. doi:10.1021/acsami.8b14745
16. Hämmerle CH, Schmid J, Lang NP, Olah AJ. Temporal dynamics of healing in rabbit cranial defects using guided bone regeneration. *J Oral Maxillofacial Surgery*. 1995;53(2):167–174. doi:10.1016/0278-2391(95)90396-8
17. Dawson DR 3rd, El-Ghannam A, Van Sickels JE, Naung NY. Tissue engineering: what is new? *Dent Clin North Am*. 2019;63(3):433–445. doi:10.1016/j.biomaterials.2018.11.008
18. Otrock ZK, Mahfouz RA, Makarem JA, Shamseddine AI. Understanding the biology of angiogenesis: review of the most important molecular mechanisms. *Blood Cells Mol Dis*. 2007;39(2):212. doi:10.1016/j.bcmd.2007.04.001
19. Lee SH, Lim P, Yoon HJ. The influence of cortical perforation on guided bone regeneration using synthetic bone substitutes: a study of rabbit cranial defects. *Int J Oral Maxillofac Implants*. 2014;29(2):464–471. doi:10.11607/jomi.3221
20. Bertl K, Domic D, Hirtler L, Heimel P, Esfandeyari A, Stavropoulos A. Micro-CT evaluation of the cortical bone micro-architecture in the anterior and posterior maxilla and the maxillary sinus floor. *Clin Oral Investig*. 2019;23(3):1453–1459. doi:10.1007/s00784-018-2573-0
21. Slotte C, Lundgren D. Impact of cortical perforations of contiguous donor bone in a guided bone augmentation procedure: an experimental study in the rabbit skull. *Clin Implant Dent Relat Res*. 2002;4(1):1–10. doi:10.1111/j.1708-8208.2002.tb00145.x
22. Gordh M, Alberius P, Lindberg L, Johnell O. Bone graft incorporation after cortical perforations of the host bed. *Otolaryngology Head Neck Surgery*. 1997;117(6):664–670. doi:10.1016/S0194-59989770050-0
23. Danesh-Sani SA, Tarnow D, Yip JK, Mojaver R. The influence of cortical bone perforation on guided bone regeneration in humans. *Int J Oral Maxillofac Surg*. 2017;46(2):261–266. doi:10.1016/j.ijom.2016.10.017
24. de Carvalho PS, Vasconcellos LW, Pi J. Influence of bed preparation on the incorporation of autogenous bone grafts: a study in dogs. *Int J Oral Maxillofacial Implants*. 2000;15(4):565–570.
25. Oda T, Kinoshita K, Ueda M. Effects of cortical bone perforation on periosteal distraction: an experimental study in the rabbit mandible. *J Oral Maxillofacial Surgery*. 2009;67(7):1478–1485. doi:10.1016/j.joms.2008.06.085
26. Van SD, Johansson C, Quirynen M, Molly L, Albrektsson T, Naert I. Bone augmentation by means of a stiff occlusive titanium barrier. *Clin Oral Implants Res*. 2003;14(1):63–71. doi:10.1034/j.1600-0501.2003.140109.x
27. Lundgren AK, Dan L, Hämmerle CHF, Nyman S, Sennerby L. Influence of decortication of the donor bone on guided bone augmentation: an experimental study in the rabbit skull bone. *Clin Oral Implants Res*. 2000;11(2):99–106. doi:10.1034/j.1600-0501.2000.00002.x
28. Rasmusson L, Sennerby L, Dan L, Nyman S. Morphological and dimensional changes after barrier removal in bone formed beyond the skeletal borders at titanium implants. A kinetic study in the rabbit tibia. *Clin Oral Implants Res*. 1997;8(2):103–116. doi:10.1034/j.1600-0501.1997.080205.x
29. Wang Q, Wang M, Lu X, et al. Effects of atomic-level nano-structured hydroxyapatite on adsorption of bone morphogenetic protein-7 and its derived peptide by computer simulation. *Sci Rep*. 2017;7(1):15152. doi:10.1038/s41598-017-15219-6
30. Patel KD, Singh RK, Mahapatra C, Lee EJ, Kim HW. Nanohybrid electro-coatings toward therapeutic implants with controlled drug delivery potential for bone regeneration. *J Biomed Nanotechnol*. 2016;12(10):1876–1889. doi:10.1166/jbn.2016.2301
31. da Silva Brum I, de Carvalho JJ, da Silva Pires JL, de Carvalho MAA, Dos Santos LBF. Nanosized hydroxyapatite and β-tricalcium phosphate composite: physico-chemical, cytotoxicity, morphological properties and in vivo trial. *Sci Rep*. 2019;9(1):19602. doi:10.1038/s41598-019-56124-4
32. Lee MS, Lee DH, Jeon J, Oh SH. Topographically defined, biodegradable nanopatterned patches to regulate cell fate and acceleration of bone regeneration. *ACS Appl Mater Interfaces*. 2018;10(45):38780–38790. doi:10.1021/acsami.8b14745
33. Street J, Bao M, Deguzman L, et al. Vascular endothelial growth factor stimulates bone repair by promoting angiogenesis and bone turnover. *Proc Nat Acad Sci*. 2002;99(15):9656–9661. doi:10.1073/pnas.152324099
34. Mayr-Wohlfart U, Waltenberger J, Hausser H, et al. Vascular endothelial growth factor stimulates chemotactic migration of primary human osteoblasts. *Bone*. 2002;30(3):472–477. doi:10.1016/s8756-3282(01)00690-1
35. Leach JK, Kaigler D, Wang Z, Krebsbach PH, Mooney DJ. Coating of VEGF-releasing scaffolds with bioactive glass for angiogenesis and bone regeneration. *Biomaterials*. 2006;27(17):3249–3255. doi:10.1016/j.biomaterials.2006.01.033
36. Liu W, Du B, Zhou L, Wang Q, Wu J. Ultraviolet functionalization improved bone integration on titanium surfaces by fluorescent analysis in rabbit calvarium. *J Oral Implantol*. 2019;45(2):107–115. doi:10.1563/aaid-joi-D-17-00009
37. Lee JS, Lee JS. Proof-of-concept study of vertical augmentation using block-type allogenic bone grafts: A preclinical experimental study on rabbit calvaria. *J Biomed Mater Res B Appl Biomater*. 2018;106(7):2700–2707. doi:10.1002/jbm.b.34087
38. Sohn JY, Park JC, Um YJ, et al. Spontaneous healing capacity of rabbit cranial defects of various sizes. *J Periodontal Implant Sci*. 2010;40(4):180–187. doi:10.5051/jpis.2010.40.4.180
39. El Zahwy M, Taha S, Mounir R, Mounir M. Assessment of vertical ridge augmentation and marginal bone loss using autogenous onlay vs inlay grafting techniques with simultaneous implant placement in the anterior maxillary esthetic zone: A randomized clinical trial. *Clin Implant Dent Relat Res*.2019;21(6):1140–1147. doi:10.1111/cid.12849
40. Fernández-Barbero JE, Ata-Ali J, OV F, et al. Bone augmentation using autogenous bone versus biomaterial in the posterior region of atrophic mandibles: A systematic review and meta-analysis. *Clin Oral Implants Res*. 2018;76:1–8. doi:10.1111/clr.13098
41. Guskuma MH, Hochuli-Vieira E, Pereira FP, et al. Bone regeneration in surgically created defects filled with autogenous bone: an epifluorescence microscopy analysis in rats. *J Appl Oral Sci*. 2010;18(4):346–353. doi:10.1590/s1678-77572010000400005
42. Kochi G, Sato S, Ebihara H, Hirano J, Arai Y, Ito K. A comparative study of microfocus CT and histomorphometry in the evaluation of bone augmentation in rat calvarium. *J Oral Sci*. 2010;52(2):203–211. doi:10.2334/josnusd.52.203
43. Ben-Nissan B, Milev A, Vago R. Morphology of sol-gel derived nano-coated coralline hydroxyapatite. *Biomaterials*. 2004;25(20):4971–4975. doi:10.1016/j.biomaterials.2004.02.006
44. Acar AH, Alan H, zgür C, Vardi N, Asutay F, Güler I. Is more cortical bone decortication effective on guided bone augmentation? *J Craniofacial Surgery*. 2016;27(7):1. doi:10.1097/SCS.0000000000002932
45. Frost HM. The regional acceleratory phenomenon: a review. *Henry Ford Hosp Med J*. 1983;31(1):3–9.
46. Norton MR, Odell EW, Thompson ID, Cook RJ. Efficacy of bovine bone mineral for alveolar augmentation: A human histologic study. *Clin Oral Implants Res*. 2004;14(6):775–783. doi:10.1046/j.0905-7161.2003.00952.x
47. Zhou H, Lee J. Nanoscale hydroxyapatite particles for bone tissue engineering. *Acta Biomater*. 2011;7(7):2769–2781. doi:10.1016/j.actbio.2011.03.019

48. Barba A, Diez-Escudero A, Espanol M, Bonany M, Sadowska JM. Impact of biomimicry in the design of osteoinductive bone substitutes: nanoscale matters. *ACS Appl Mater Interfaces*. 2019;11(9):8818–8830. doi:10.1021/acsami.8b20749
49. Karaman S, Leppänen VM, Alitalo K. Vascular endothelial growth factor signaling in development and disease. *Development*. 2018;145:(14). doi:10.1242/dev.151019
50. Hoeben A, Landuyt B, Highley MS, Wildiers H, Van Oosterom AT, De Bruijn EA. Vascular endothelial growth factor and angiogenesis. *Development*. 2004;56(4):549–580. doi:10.1242/dev.151019
51. Yang P, Wang C, Shi Z, et al. rhVEGF 165 delivered in a porous beta-tricalcium phosphate scaffold accelerates bridging of critical-sized defects in rabbit radii. *J Biomed Mater Res A*. 2010;92(2):626–640. doi:10.1002/jbm.a.32403
52. Spyridopoulos I, Brogi E, Kearney M, et al. Vascular endothelial growth factor inhibits endothelial cell apoptosis induced by tumor necrosis factor-alpha: balance between growth and death signals. *J Mol Cell Cardiol*. 1997;29(5):1321–1330. doi:10.1006/jmcc.1996.0365
53. Koch S, Tugues S, Li X, Gualandi L, Claesson-Welsh L. Signal transduction by vascular endothelial growth factor receptors. *Biochem J*. 2011;437(2):169–183. doi:10.1042/bj20110301
54. Thiagarajan L, Dixon JE, Tozzi G, Oreffo ROC, Clarkin CE, Gerstenfeld LC. VEGF and bone cell signalling: an essential vessel for communication? *Sci Rep*. 2013;31(1):1–11. doi:10.1038/s41598-019-53249-4
55. Slotte C, Lundgren D, Sennerby L. Bone morphology and vascularization of untreated and guided bone augmentation-treated rabbit calvaria: evaluation of an augmentation model. *Clin Oral Implants Res*. 2005;16(2):228–235. doi:10.1111/j.1600-0501.2004.01098.x
56. Dong X, Wang Q, Wu T, Pan H. Understanding adsorption-desorption dynamics of BMP-2 on hydroxyapatite (001) surface. *Biophys J*. 2007;93(3):750–759. doi:10.1529/biophysj.106.103168